thermo scientific

APPLICATION NOTE 21850

# Comparability study for the determination of post-translational modifications of biotherapeutic drug products and biosimilars by automated peptide mapping analysis


## Authors

Silvia Millán-Martín, Izabela Zaborowska, Craig Jakes, Sara Carillo, Jonathan Bones
Characterisation and Comparability Laboratory, NIBRT – The National Institute for Bioprocessing Research and Training, Dublin, Ireland



## Keywords

NIBRT, biopharmaceuticals, biotherapeutics, biosimilars, follow-on biologic, comparability studies, CQAs, monoclonal antibodies (mAbs), chimeric IgG1, humanized IgG1, rituximab, trastuzumab, post-translational modifications (PTMs), peptide mapping, bottom-up, high throughput, Magnetic SMART Digest kit, KingFisher Duo Prime Purification System, Vanquish Flex Binary UHPLC System, Acclaim VANQUISH C18 column, Q Exactive Plus Hybrid Quadrupole-Orbitrap mass spectrometer


## Application benefits

- Rapid, automated sample preparation within 1 hour leading to highly reproducible results for innovator and biosimilar comparability studies, with less hands-on time
- Simple protein digestion with minimal user intervention for peptide mapping analysis
- High confidence in results with excellent data quality; approximately 100% sequence coverage and low levels of sample preparation induced post-translational modifications

## Goal

The characterization of biosimilarity is required to demonstrate the presence or absence of differences resulting from the manufacturing process by investigating the physicochemical and biological properties of a biosimilar molecule compared to the corresponding reference product (innovator). In this study peptide mapping was used to evaluate the similarity of post-translational modifications (PTMs) detected in rituximab and trastuzumab drug products and their respective biosimilars. To automate and speed up the method we used Thermo Scientific™ Magnetic SMART Digest™ on a Thermo Scientific™ KingFisher™ Duo Prime Purification System. The efficiency and reproducibility of the platform was evaluated with a specific focus on the determination

nibrt National Institute for Bioprocessing Research and Training

ThermoFisher SCIENTIFIC

of protein sequence coverage and identification of PTMs including deamidation, oxidation, lysine clipping, glycation, and glycosylation.

## Introduction

A biosimilar is a biological medicine that contains essentially the same active substance as the original reference product whose patent had expired. Biosimilars must be produced in accordance with the specific requirements established by the European Medicine Agency (EMA) and other regulatory agencies to ensure their biosimilarity to the reference product in terms of efficacy, quality and safety.[1]

The biosimilar market has grown exponentially since the approval of the first marketing authorization for a biosimilar (somatropin) by the EMA in 2006. In fact, 30% to 50% of new drugs approved in Europe are estimated to be biosimilars.[2] In 2013, the first monoclonal antibody (mAb) biosimilar, infliximab, was approved in Europe.[3] The EMA requirements to approve biosimilars vary according to the class of molecule, and decisions occur case by case.

MAbs are complex biological molecules. As a result, the studies required to prove biosimilarity are much more challenging than those requested for generic small molecule drugs. The intricate structure of biological medicinal products and the complex nature of their manufacturing process in living organisms impose a separate, and more stringent, regulatory approval process. This is very important in quality terms since an extensive physicochemical characterization and comparison of innovative products and the proposed biosimilar should be performed. Thus, a multitude of analytical techniques should be used to compare the biosimilar versus the reference medicinal product through a "comparability exercise".[4,5]

Details of the production of biologic products vary from batch to batch and with any manufacturing change that can occur for different reasons, including scaling-up the process to address commercial demand, improving the efficiency of the process, and modernizing the process when major equipment needs to be replaced or updated. The available comparability protocols allow for these changes to occur, and in the same way, provide support for the biosimilar evolution. The first step in developing a biosimilar is to carefully examine multiple samples of the reference product to determine how variable this product is over time during its shelf life, between batches and manufacturing sites.[6]

Similarity between a proposed biosimilar and innovator can be affected by many factors. MAbs exist as a series of heterogeneous variants due to PTMs that arise during cell culture, purification, and storage. Extensive analytical testing platforms are needed for in-depth characterization and to ensure product stability and proper in-process controls to guarantee patient safety. During the development and production of therapeutic mAbs, characterization of structural variants is a critical challenge. The rigors of biotherapeutic development and analysis have clearly indicated a need for control over every stage of development. The biopharmaceutical industry requires fast and robust analytical platforms to fulfil regulatory requirements involved in the Biologics License Applications (BLA) process.

Rituximab is a genetically engineered chimeric murine/human mAb directed against the CD20 antigen found on the surface of normal and malignant B lymphocytes. The antibody is an IgG1 kappa immunoglobulin containing murine light- and heavy-chain variable region sequences and human constant region sequences. Rituximab is composed of two heavy chains of 451 amino acids and two light chains of 213 amino acids. The originator product, MabThera/Rituxan™ (rituximab), was approved by the U.S. Food and Drug Administration (FDA) in November 1997 and by the European Medicines Agency (EMA) in June 1998.[7] The patents on MabThera/Rituxan expired in the U.S. in September 2016 and in Europe in February 2013. Some of the rituximab biosimilars are Truxima™, approved by EC in February 2017, and Blitzima™, Ritemvia™, and Rituzena (previously Tuxella), approved by EC in July 2017.

Trastuzumab (Herceptin™) is a recombinant IgG1 kappa, humanized mAb that selectively binds with high affinity in a cell-based assay to the extracellular domain of the human epidermal growth factor receptor protein, produced in CHO cell culture. Herceptin received approval from the FDA in 1998.[8] In December 2017, the FDA approved Ogivri™ (trastuzumab-dkst) as a biosimilar to Herceptin for the treatment of patients with breast or metastatic stomach cancer (gastric or gastroesophageal junction adenocarcinoma) whose tumors overexpress the HER2 gene (HER2+). It displays biosimilar properties as Herceptin according to clinical data. While Ogivri is the first biosimilar approved in the U.S. for the treatment of breast cancer or stomach cancer, it is the second biosimilar approved in the U.S. for the treatment of cancer.

This application note presents the benefits of using the recently developed Magnetic SMART Digest Kit to perform a comparability study of PTMs for rituximab and trastuzumab innovators and biosimilars. An efficient approach that combines automated enzymatic digestion using the Magnetic SMART Digest resin option on a KingFisher Duo Prime Purification System, in combination with the high-resolution, accurate-mass (HRAM) capabilities of the Thermo Scientific™ Q Exactive™ hybrid quadrupole-Orbitrap mass spectrometer. High-resolution chromatographic separation with the Thermo Scientific™ Vanquish™ Flex UHPLC system using a Thermo Scientific™ Acclaim™ VANQUISH™ C18, provided high quality reproducible data. Thermo Scientific™ BioPharma Finder™ software was used to interrogate the data sets.

## Experimental

### Consumables

- Deionized water, 18.2 MΩ·cm resistivity
- Water, Optima™ LC/MS grade (Fisher Chemical) (P/N 10505904)
- Acetonitrile, Optima™ LC/MS grade (Fisher Chemical) (P/N 10001334)
- Water with 0.1% formic acid (v/v), Optima™ LC/MS grade (Fisher Chemical) (P/N 101881640
- Acetonitrile with 0.1% formic acid (v/v), Optima™ LC/MS grade (Fisher Chemical) (P/N 10118464)
- Trifluoroacetic acid (TFA) (Fisher Chemical) (P/N 10294110)
- Thermo Scientific™ SMART Digest™ Trypsin Kit, Magnetic Bulk Resin option (P/N 60109-101-MB)
- Thermo Scientific™ Pierce™ DTT (Dithiothreitol), No-Weigh™ Format (P/N 20291)
- Iodoacetic acid, sodium salt 99% (IA) (Acros Organics™) (P/N 10235940)
- Thermo Scientific™ KingFisher™ Deepwell, 96 well plate (P/N 95040450)
- Thermo Scientific™ KingFisher™ Duo 12-tip comb (P/N 97003500)
- Acclaim VANQUISH C18 column, 2.2 µm, 2.1 x 250 mm (P/N 074812-V)
- Thermo Scientific™ Virtuoso™ vial, clear 2 mL kit with septa and cap (P/N 60180-VT405)
- Thermo Scientific™ Virtuoso™ vial identification system (P/N 60180-VT100)

### Equipment

- KingFisher Duo Prime Purification System (P/N 5400110

Vanquish Flex Binary UHPLC System including:

- Binary Pump F (P/N VF-P10-A)
- Column Compartment H (P/N VH-C10-A)
- Split Sampler FT (P/N VF-A10-A)
- System Base Vanquish Horizon (P/N VH-S01-A)

Q Exactive Plus Hybrid Quadrupole-Orbitrap Mass Spectrometer (P/N IQLAAEGAAPFALGMBDK)

Thermo Scientific™ Nanodrop™ 2000 Spectrophotometer (P/N ND-2000)

### Sample preparation

Commercially available rituximab and trastuzumab mAb drug products (DP) were supplied at different concentrations and two biosimilars (BS) were produced in-house using CHO expression systems (Table 1).

Monoclonal antibody samples were prepared in triplicate.

**Table 1. Monoclonal antibodies used in the study**

| Drug | Specifications | Concentration | Type |
|---|---|---|---|
| Rituximab DP | CHO cells | 10 mg/mL | Recombinant chimeric IgG1 mAb |
| Rituximab BS | In-house CHO expressed | 3.1 mg/mL | Recombinant chimeric IgG1 mAb |
| Trastuzumab DP | CHO cells | 21 mg/mL | Recombinant humanized IgG1 mAb |
| Trastuzumab BS | In-house CHO expressed | 3.2 mg/mL | Recombinant humanized IgG1 mAb |

### Rituximab/trastuzumab biosimilars in-house production

ExpiCHO-S™ Cells (Gibco™, P/N A29127) were derived from a non-engineered subclone that has been screened and isolated from Chinese hamster ovary (CHO) cells. Cells were cultured in suspension in serum-free, chemically defined media (Gibco), and transiently transfected with plasmid DNA encoding particular mAb using lipid-based transfection system (Gibco). The vectors (pFUSEss-CHIg-hG1 and pFUSE2ss-CLIg-hk) were purchased from Invivogen. Following transfection, the cells were harvested, and samples of clarified media were passed through a HiTrap™ Protein A column then washed with phosphate buffered saline before elution of mAb from the Protein A column using 100 mM citric acid, pH 3.2. MAb solutions were buffer exchanged in phosphate buffered saline, and protein concentration was evaluated with a Nanodrop 2000 Spectrophotometer.

**Table 2. KingFisher Duo Prime plate layout utilized for sample preparation. Reagents and associated volumes placed in each well are outlined.**

| Lane | Content | Volume Applied to Each Well (µL) |
|---|---|---|
| A | SMART Digest buffer | 150 |
| | Sample (2 mg/mL) | 50 |
| B | Tip Comb | |
| C | Empty | |
| D | Magnetic SMART Beads | 15 |
| | Bead Buffer (SMART Digest buffer) | 100 |
| E | Bead Wash Buffer (SMART Digest buffer 1:4 (v/v)) | 200 |
| F | Waste Lane (Water) | 250 |

**Table 3. Protocol for automated peptide mapping using a KingFisher Duo Prime system**

| Step | Release Bead | Mixing | Collect Beads | Temp | Lane |
|---|---|---|---|---|---|
| Collect Bead | – | 10 s Bottom Mix | 3 count, 1 s | – | D |
| Bead Wash | Yes | 1 min Medium Mix | 3 count, 1 s | – | E |
| Digest and Cool | Yes | 45 min Medium Mix | 3 count, 15 s | 70 °C heating while mixing<br>10 °C post temperature | A |
| Release Beads | Yes, Fast | – | – | – | F |

### Protocol for sample preparation using a SMART Digest trypsin kit, magnetic bulk resin option (Magnetic SMART Digest)

Samples were diluted to 2 mg/mL in water. For each sample digest, sample and buffers were added to each lane of a KingFisher Deepwell 96 well plate as outlined in Table 2. Bead "wash buffer" was prepared by diluting SMART Digest buffer 1:4 (v/v) in water. Bead buffer was neat SMART Digest buffer. Digestion was performed using the Kingfisher Duo Prime Purification System with Thermo Scientific™ BindIt™ software (version 4.0), using the protocol outlined in Table 3. Samples were incubated for 45 minutes at 70 °C on medium mixing speed (to prevent sedimentation of beads), with post-digestion cooling carried out to 10 °C. Following digestion, disulfide bond reduction was performed with 10 mM DTT for 30 minutes at 57 °C and subsequently alkylated with 20 mM IA in darkness for 30 minutes. The reaction was quenched with 15.45 µL of 100 mM DTT followed by 15.64 µL of 10% TFA (final concentration 11 mM DTT and 1% TFA).

Finally 3 µg for each sample were loaded on the column for all runs.

### LC conditions

| | |
|---|---|
| Column: | Acclaim VANQUISH C18, 2.2 µm, 2.1 × 250 mm |
| Mobile phase A: | 0.1% formic acid aqueous solution |
| Mobile phase B: | 0.1% formic acid solution in acetonitrile |
| Flow rate: | 0.3 mL/min |
| Column temperature: | 25 °C (Still air mode) |
| Autosampler temperature: | 5 °C |
| Injection volume: | 10 µL |
| Injection wash solvent: | MeOH:$H_2O$, 10:90 |
| Needle wash: | Enabled pre-injection |
| Gradient: | Table 4 for details |

Table 4. Mobile phase gradient for UHPLC separation of peptides

| Time (minutes) | Flow (mL/min) | % Mobile Phase B | Curve |
|---|---|---|---|
| 0.000 | 0.300 | 2.0 | 5 |
| 45.000 | 0.300 | 40.0 | 5 |
| 46.000 | 0.300 | 80.0 | 5 |
| 50.000 | 0.300 | 80.0 | 5 |
| 50.500 | 0.300 | 2.0 | 5 |
| 65.000 | 0.300 | 2.0 | 5 |

## MS Conditions

Detailed MS method parameters are shown in Tables 5 and 6.

Table 5. MS source and analyzer conditions

| MS Source Parameters | Setting |
|---|---|
| Source | Thermo Scientific™ Ion Max source with HESI-II probe |
| Sheath Gas Pressure | 40 psi |
| Auxiliary Gas Flow | 10 arbitrary units |
| Probe Heater Temperature | 400 °C |
| Source Voltage | 3.8 kV |
| Capillary Temperature | 300 °C |
| S-lens RF Voltage | 50 V |

Table 6. MS method parameters utilized for peptide mapping analysis

| General | Setting | $MS^2$ Parameters | Setting |
|---|---|---|---|
| Run Time | 0 to 65 min | Resolution Settings | 17,500 |
| Polarity | Positive | AGC Target Value | $1.0 \times 10^5$ |
| **Full MS Parameters** | **Setting** | Isolation Width | 2.0 *m/z* |
| Full MS Mass Range | 200–2,000 *m/z* | Signal Threshold | $1.0 \times 10^4$ |
| Resolution Settings | 70,000 | Normalized Collision Energy (HCD) | 28 |
| AGC Target Value | $3.0 \times 10^6$ | Top-N $MS^2$ | 5 |
| Max Injection Time | 100 ms | Max Injection Time | 200 ms |
| Default Charge State | 2 | Fixed First Mass | – |
| SID | 0 eV | Dynamic Exclusion | 7.0 s |
| Microscans | 1 | Loop Count | 5 |

## Data processing

Thermo Scientific™ Xcalibur™ software version 4.0.27.13 (Cat. No. OPTON-30487) was used for data acquisition and analysis. For data processing, Thermo Scientific™ BioPharma Finder™ software version 3.0 was applied. Detailed parameter settings are shown in Table 7.

Table 7. Biopharma Finder 3.0 software parameter settings for analysis of peptide mapping data

| Component Detection | Setting |
|---|---|
| Absolute MS Signal Threshold | 8.0 x $10^4$ counts |
| Typical Chromatographic Peak Width | 0.3 |
| Relative MS Signal Threshold (% base peak) | 1.00 |
| Relative Analog Threshold (% of highest peak) | 1.00 |
| Width of Gaussian Filter (represented as 1/n of chromatographic peak width) | 3 |
| Minimum Valley to Be Considered as Two Chromatographic Peaks (%) | 80.0 |
| Minimum MS Peak Width (Da) | 1.2 |
| Maximum MS Peak Width (Da) | 4.2 |
| Mass Tolerance (ppm for high-res or Da for low-res) | 4.00 |
| Maximum Retention Time Shift (min) | 1.69 |
| Maximum Mass (Da) | 30,000 |
| Mass Centroiding Cutoff (% from base) | 15 |
| **Identification** | **Setting** |
| Maximum Peptide Mass | 7,000 |
| Mass Accuracy | 5 ppm |
| Minimum Confidence | 0.8 |
| Maximum Number of Modifications for a Peptide | 1 |
| Unspecified Modification | -58 to +162 Da |
| N-Glycosylation | CHO |
| Protease Specificity | High |
| **Static Modifications** | **Setting** |
| Side Chain | Carboxymethylation |
| **Variable Modifications** | **Setting** |
| N Terminal | Gln→Pyro Glu |
| C Terminal | Loss of lysine |
| Side Chain | Deamidation (N)<br>Deamidation(Q)<br>Glycation (K)<br>Oxidation (MW) |

## Results and discussion

Many patents for the first biologicals derived from recombinant technology and, more recently, mAbs are expiring. Biosimilars are becoming an increasingly important area of interest for the pharmaceutical industry worldwide.[9]

The EU pioneered the development of regulatory aspects for biosimilars and associated marketing authorization, starting from the first-generation biologics (somatropin) up to complex molecules such as erythropoietin and mAbs (infliximab). EMA published a general framework guideline for biosimilars in 2005[10] introducing the principles of biosimilarity. Technological changes that occurred afterwards and the experience gained by application reviews led to an updated draft guideline released in 2013 and adopted by the Committee for Medicinal Products for Human Use (CHMP) in October 2014.

Two candidate biosimilars of rituximab and trastuzumab mAbs were compared to two commercially available chimeric and humanized IgG1 products by peptide mapping analysis using the magnetic SMART Digest kit in combination with the KingFisher Duo Prime system.

Subsequent LC/MS analysis of the generated peptides provided a powerful method for PTMs characterization to ensure mAb quality.

A peptide map is a fingerprint of a protein and the end product of several processes that provide a comprehensive understanding of the protein being analyzed. Peptide mapping is a routine analysis for the characterization of mAbs, however, it often involves tedious sample preparation steps, which might reduce reproducibility due to differences among techniques, technicians, or different partner labs. This variation can be specially challenging when it is necessary to compare different product batches or biosimilar products across months or years. As the data quality is imperative, variation in results might jeopardize product quality, ultimately affecting product efficacy and safety.

Using the Magnetic SMART Digest kit in combination with the KingFisher Duo Prime system automates the digestion process and reduces the time needed for peptide mapping sample preparation. This methodology provides significant improvements in reproducibility and method transfer over existing protocols. This results in fewer sample failures, higher throughput, and the ability to more easily interrogate data. The following figures (Figures 1 and 2) show two chromatograms of peptides from rituximab and trastuzumab drug products and biosimilars, respectively, digested with the Magnetic SMART Digest kit. Although the base peak chromatograms obtained are similar, there are distinct differences in terms of peak relative abundance and number of detected peaks. Each protein to be mapped presents unique characteristics that must be well understood so that the validated development of a peptide map provides sufficient specificity for characterization.

Rituximab and trastuzumab drug products (DP) and rituximab biosimilar (BS) can be identified with 100% sequence coverage. Trastuzumab BS is identified with 100% sequence coverage for HC and 98.60% for LC (Table 8). The missing peptide corresponds to a tripeptide 2:E143-K145 (sequence EAK), which has probably not been detected due to poor column retention and low intensity signals where confirmatory MS2 data could not be obtained.

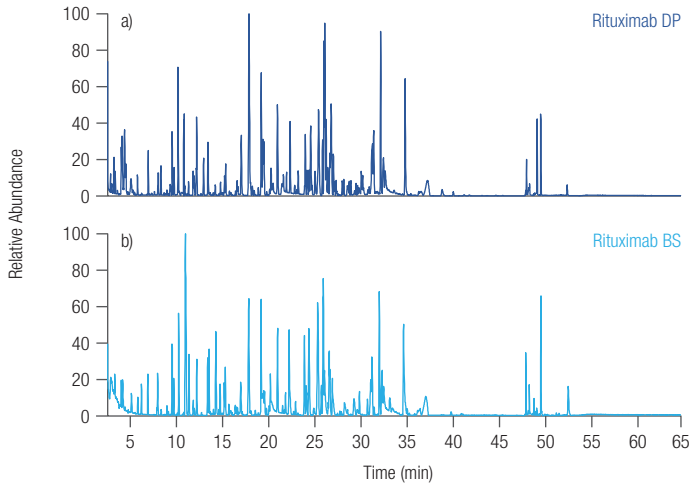


**Figure 1. Base peak chromatograms (BPCs) obtained from peptide mapping experiments of a) Rituximab DP and b) Rituximab BS In-house CHO expressed, after Magnetic SMART digestion with the KingFisher Duo Prime system**

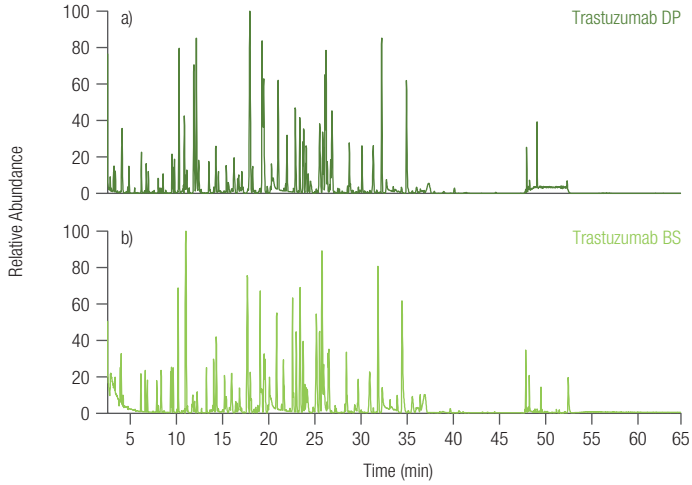


**Figure 2. BPCs obtained from peptide mapping experiments of a) Trastuzumab DP and b) Trastuzumab BS In-house CHO expressed, after Magnetic SMART digestion with the KingFisher Duo Prime system**

**Table 8. Sequence coverage for the studied recombinant IgG1 mAbs**

| Proteins | Sample | Number of Peaks | Sequence Coverage (%) |
|---|---|---|---|
| Heavy chain | Rituximab DP | 1187 | 100.00 |
| | Rituximab BS | 747 | 100.00 |
| | Trastuzumab DP | 1169 | 100.00 |
| | Trastuzumab BS | 841 | 100.00 |
| Light chain | Rituximab DP | 532 | 100.00 |
| | Rituximab BS | 378 | 100.00 |
| | Trastuzumab DP | 375 | 100.00 |
| | Trastuzumab BS | 368 | 98.60 |

A sequence coverage map (Figures 3 and 4) shows the overlap of the different peptides identified with different intensities and the different lengths due to missed cleavages. An example sequence coverage map is shown for trastuzumab DP and trastuzumab BS.

### Trastuzumab heavy chain

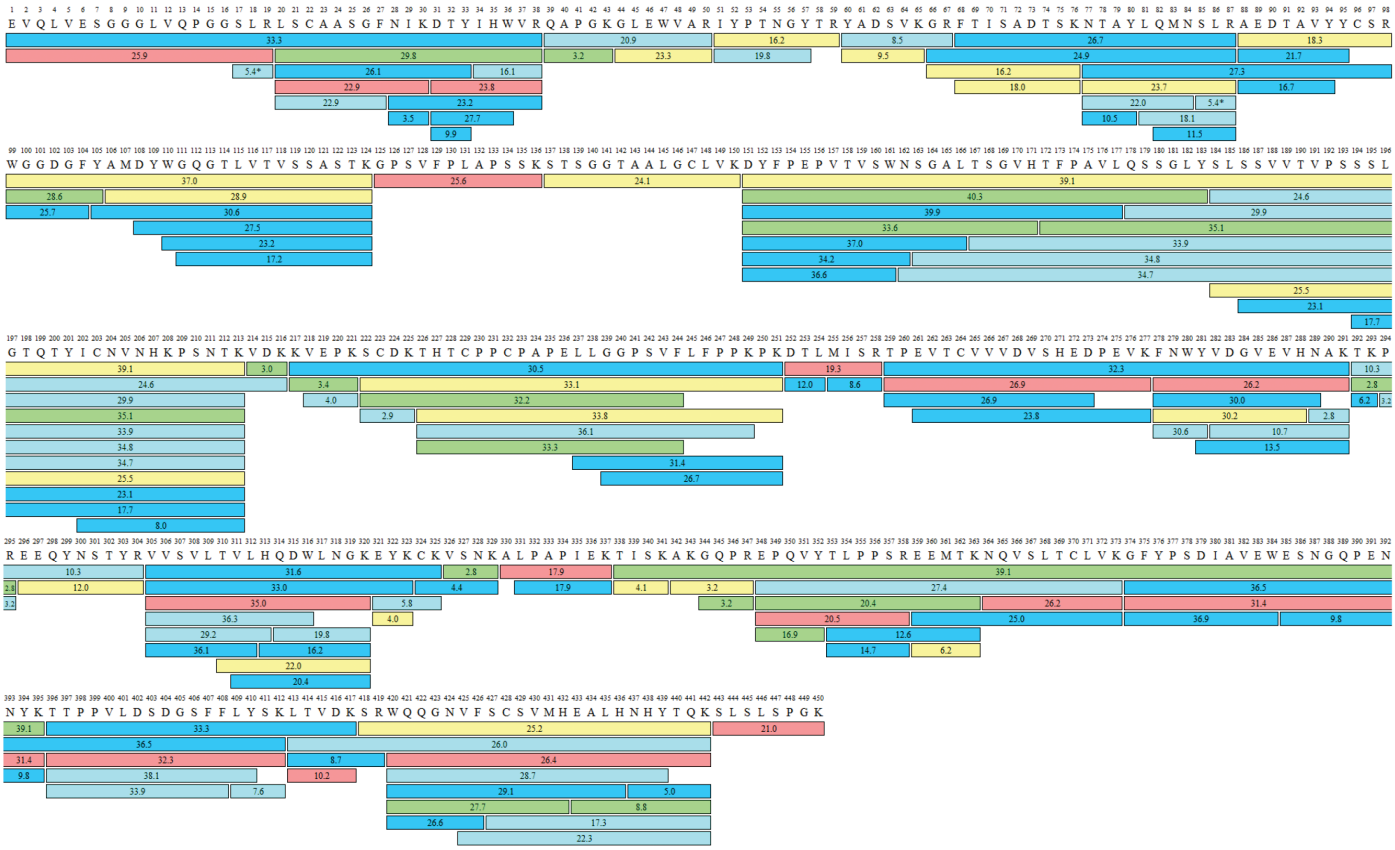


### Trastuzumab light chain

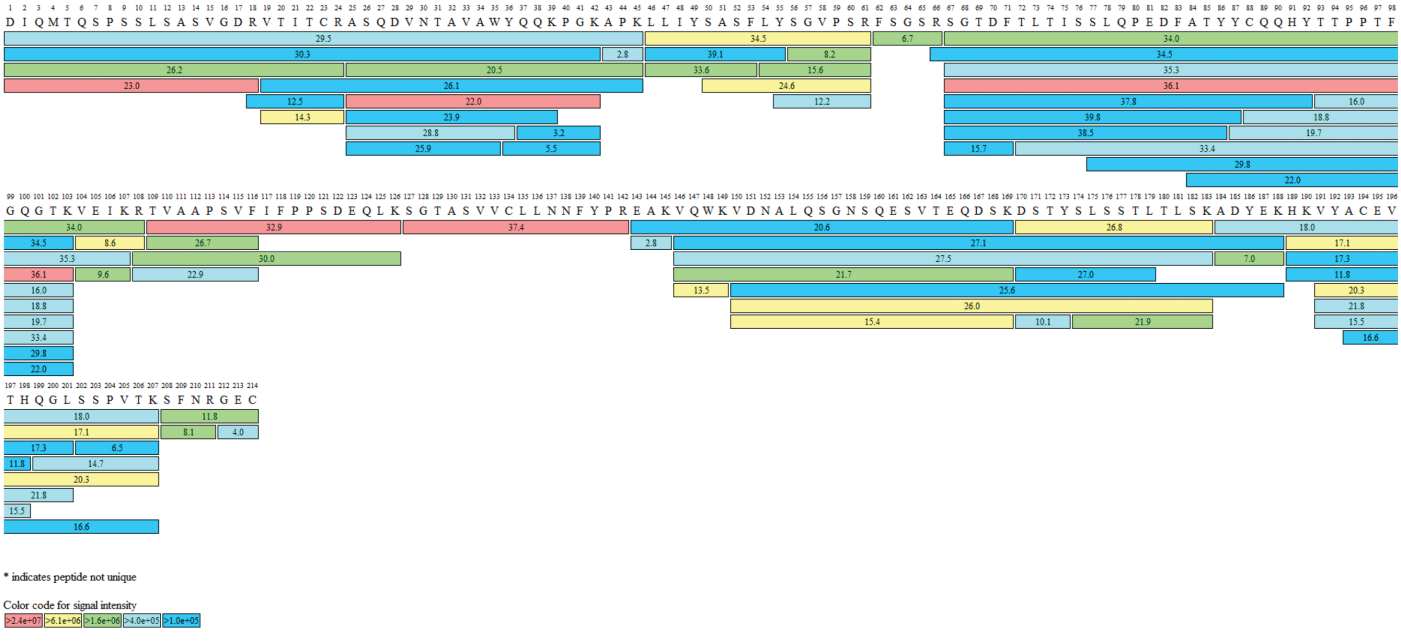


* indicates peptide not unique

Color code for signal intensity

>2.4e+07 | >6.1e+06 | >1.6e+06 | >4.0e+05 | >1.0e+05

**Figure 3. Sequence coverage map of trastuzumab DP heavy (top) and light chain (bottom), obtained using 65 min gradient for peptide separation on an Acclaim VANQUISH C18, 2.2 µm, 2.1 × 250 mm column.** The colored bars show the identified peptides, with the number in the bars reflecting the retention time (min) and the intensity of the peptide in the MS1 scan: red = high abundant >2.4e+07, yellow >6.1e+06, green >1.6e+06, light blue >4.0+05, cyan=low abundant >1.0e+05.

HerceptinBS heavy chain

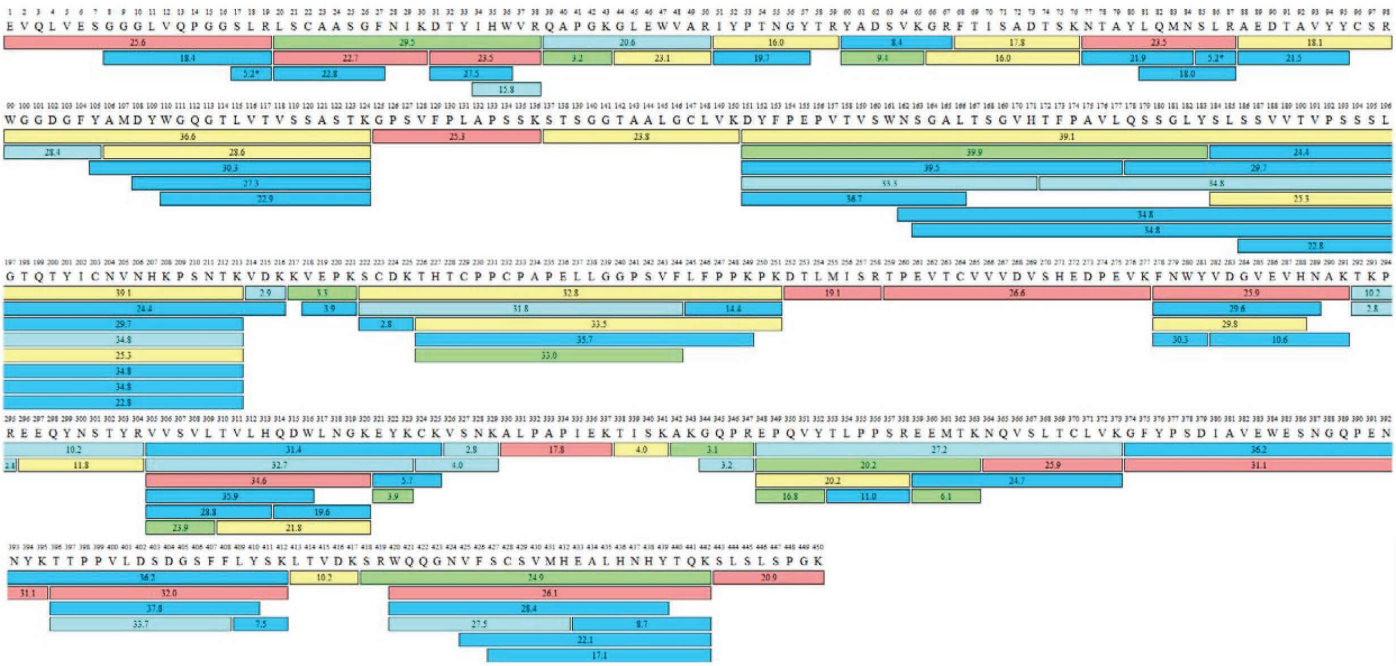


HerceptinBS light chain

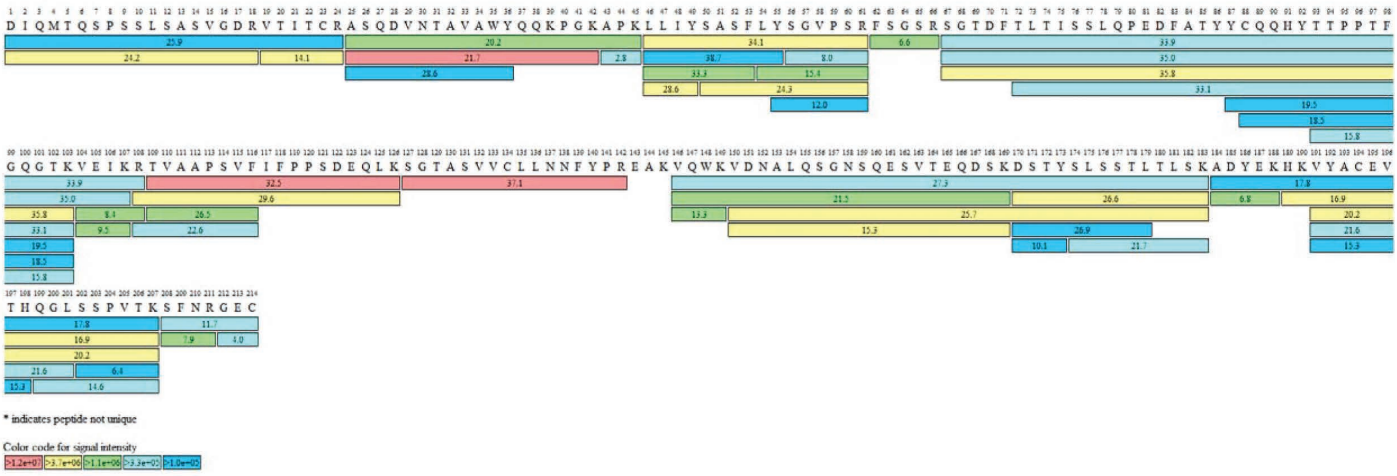


**Figure 4. Sequence coverage map of trastuzumab BS heavy (top) and light chain (bottom), obtained using 65 min gradient for peptide separation on an Acclaim VANQUISH C18, 2.2 µm, 2.1 x 250 mm column.** The colored bars show the identified peptides, with the number in the bars reflecting the retention time (min) and the intensity of the peptide in the MS1 scan: red = high abundant >1.2e+07, yellow >3.7e+06, green >1.1e+06, light blue >3.3+05, cyan=low abundant >1.0e+05.

In regard to the peptide identification with high confidence, all matched peptides were expected to have ≤5 ppm and ≥-5 ppm of MS mass error, confidence score ≥ 95, and confirmatory MS/MS spectra. Figures 5 and 6 show examples of a few single ion chromatograms (SIC) and corresponding MS/MS spectra for selected peptides present in both rituximab BS and DP, which elute at different retention times. The combination of high-quality MS and MS/MS data provides a more positive peptide match. It can be easily seen from individual peptide MS/MS fragment coverage maps that the peptides are identical in the BS and DP products.

The fragment coverage map displays the peptide sequence with corresponding modification and charge state, the average structural resolution score in number of residues (*total number of amino acids/number of peptide fragments*), and the peptide sequence with the numbered amino acid sequence and the identified fragment lines. Finally, a graphic showing the identified fragment ions using a color code for ion intensity (red, yellow, green, cyan, and blue, with red as most intense and blue as the least intense) is also displayed for each SIC example.

The experimental spectrum plots are also shown on the right side for each SIC. An inverted triangle marker at the top of the spectral line represents the theoretical precursor ion. The labels appear in color for the identified peaks and show their fragment ion assignments and charge states (for example, “y1”, “b2”, or “M”). The color for the lines and labels for the identified ions in the experimental spectrum vary based on the ion type, as follows:

- Light blue for a ions with a charge on the N-terminal side
- Dark blue for b ions with a charge on the N-terminal side
- Red for y ions with a charge on the C-terminal side
- Orange for x ions with a charge on the C-terminal side

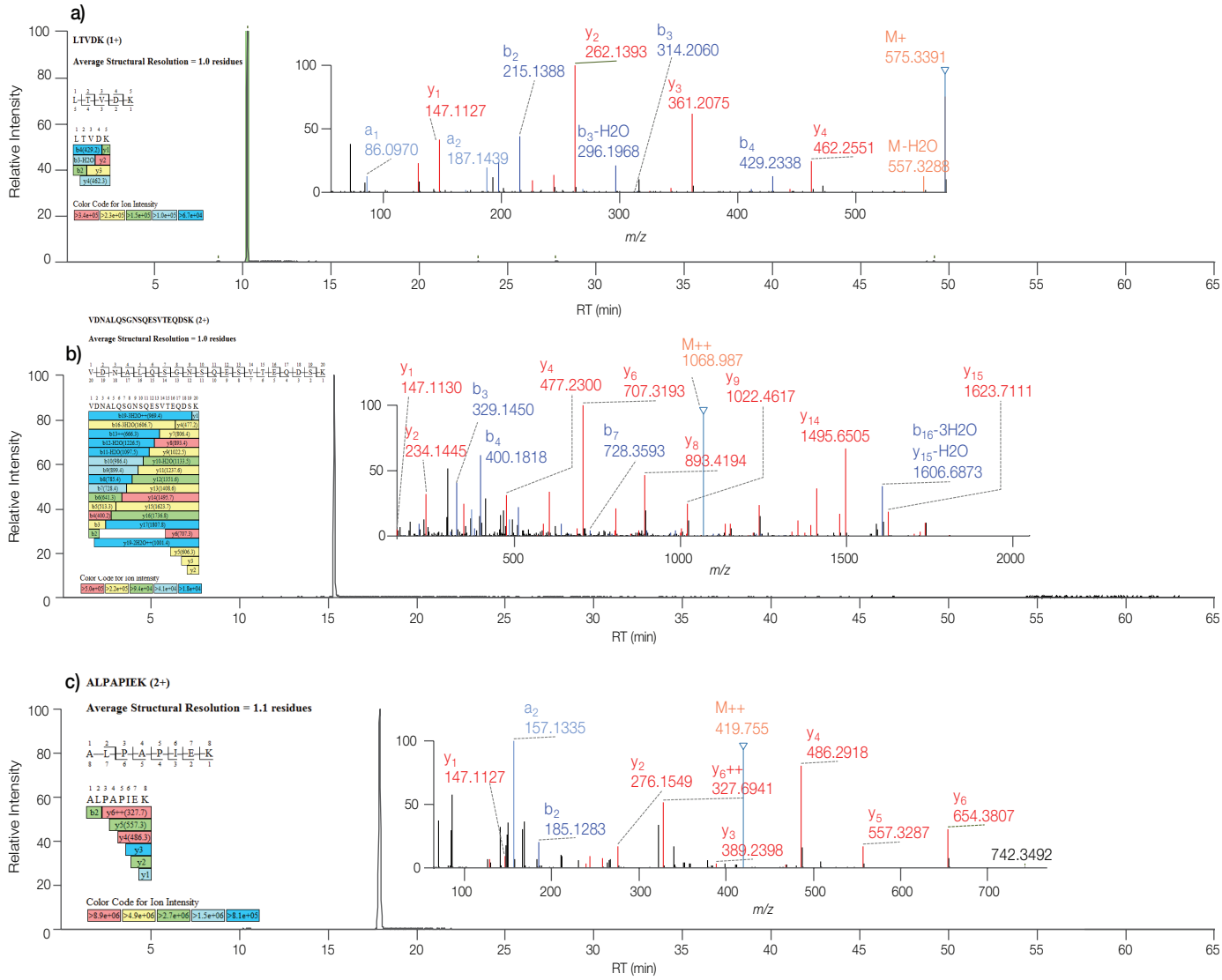


**Figure 5. Representative SICs for digested Rituximab BS, MS/MS spectra and fragment coverage map of peptides (a) 1:L414-K418, (b) 2:V149-K168, (c) 1:A331-K338**

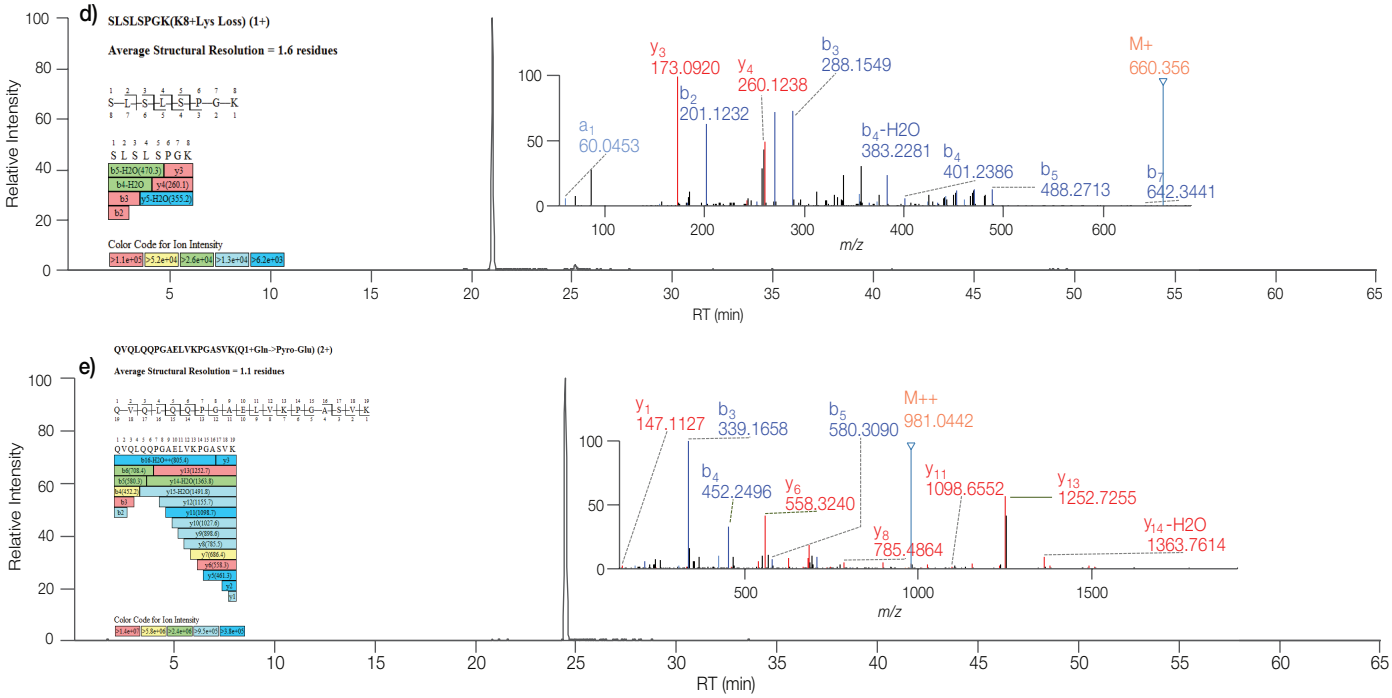


Figure 5 (continued). Representative SICs for digested Rituximab BS, MS/MS spectra and fragment coverage map of peptides (d) 1:S444-K451, and (e) 1:Q1-K19

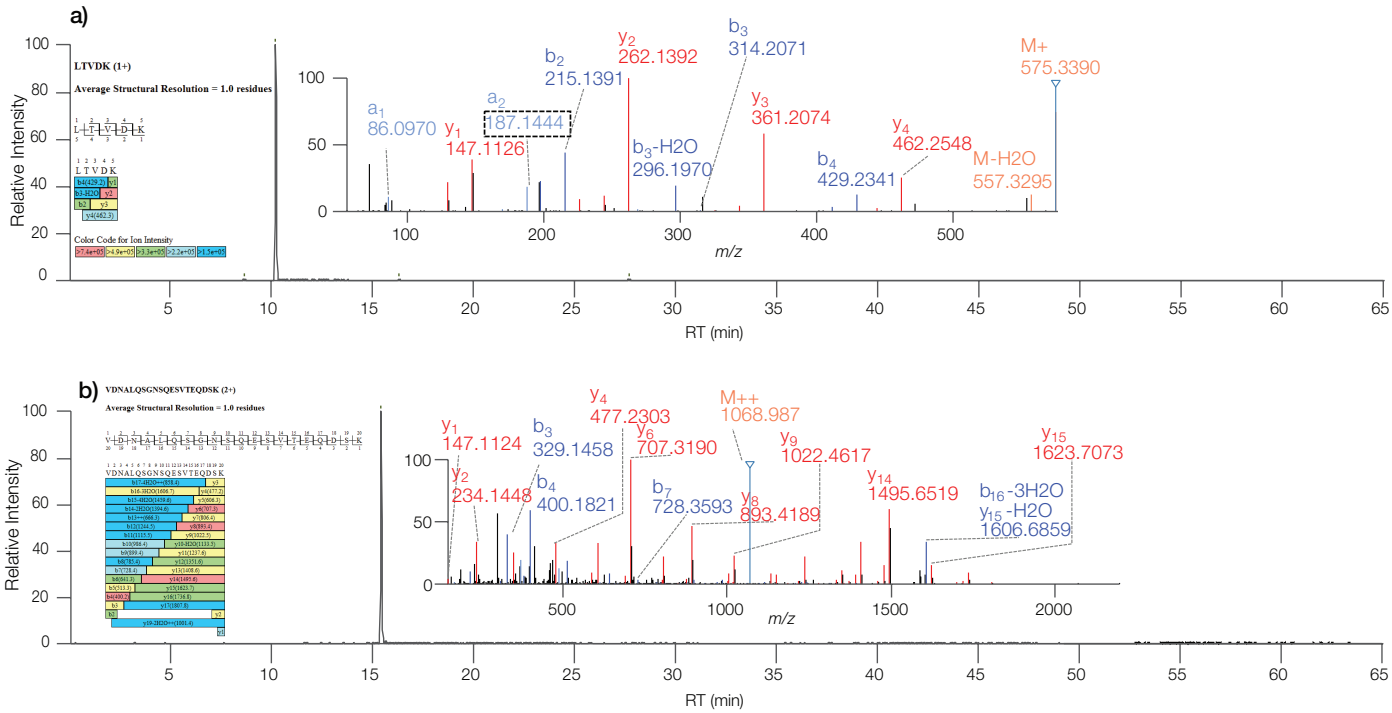


Figure 6. Representative SICs form digested Rituximab DP, MS/MS spectra and fragment coverage map of peptides (a) 1:L414-K418, (b) 2:V149-K168

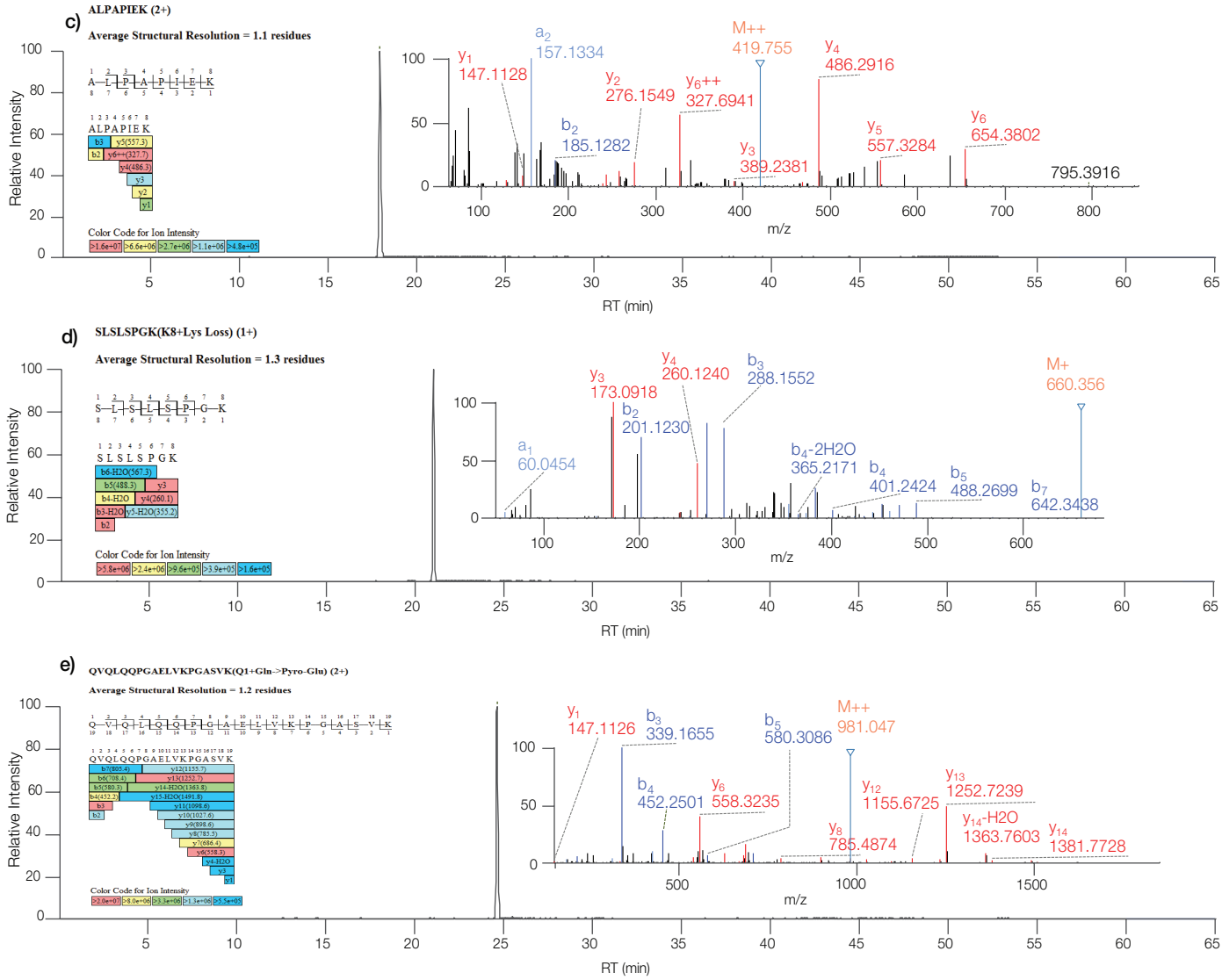


**Figure 6 (continued). Representative SICs form digested rituximab DP, MS/MS spectra and fragment coverage map of peptides (c) 1:A331-K338, (d) 1:S444-K451, and (e) 1:Q1-K19**

Peptide mapping analysis also facilitates identification and quantitation of PTMs. Many common PTMs cause a shift in reversed-phase LC retention relative to the native peptide, and in combination with direct MS and MS/MS analysis it can be used to interrogate modifications with relatively large mass shifts, such as C-terminal lysine (128 Da), glycation (162 Da), and small mass differences such as deamidation (1 Da), oxidation (16 Da), from other peptide.

Tables 9 and 10 summarize the identification and relative quantification of a subset of monitored modifications across the rituximab and trastuzumab innovator and biosimilar candidates, respectively. PTMs such as deamidation, oxidation, glycation, C-terminal lysine clipping, and glycosylation are confidently identified based on MS1 and MS/MS spectra. A tilde (~) before the modification in the table indicates the modification was found on the parent tryptic peptide but could not be localized on a specific amino acid with MS/MS spectra. The relative abundance of the detected modifications in the four mAb products has a relative standard deviation < 10% in the majority of cases. Overall, the method shows that important information regarding PTMs can be obtained reproducibly and accurately.

Deamidation of asparagine (Asn, N)[11] and glutamine (Gln, Q)[12] residues is a common degradation of proteins and can significantly impact protein structure and function. The rate of deamidation depends on protein sequence and conformation, as well as on external factors such as temperature, pH, and time. Figure 7 shows the average relative abundance of nine of the most abundant deamidation modifications for the studied

mAbs. Both drug products contain measurable levels of deamidation and a few common deamidation sites were observed for the residues N55, N319/N318, N393/N392, and N136/N137. For rituximab, the highest levels were detected for N55, with levels of 7.07% for DP and 8.57% for BS. Trastuzumab showed the highest deamidation levels on Q27, only detected for the DP (6.63%). Trastuzumab also showed high deamidation levels on the N30 residue of the LC for both DP and BS (3.09% and 9.39%, respectively).

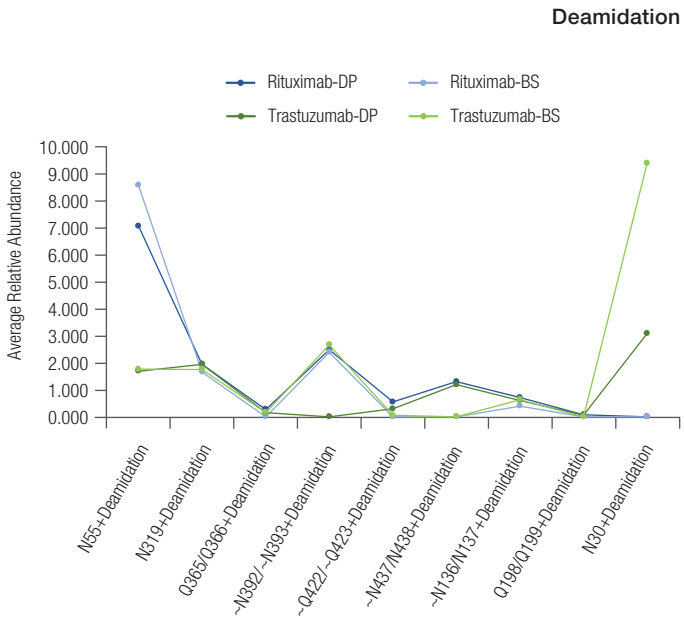


**Figure 7. Average relative abundance (n=3) of 11 identified deamidation modifications for rituximab and trastuzumab drug products and biosimilars produced in-house by CHO expression systems**

Microheterogeneity can sometimes be attributed to oxidation of tryptophan (Trp, W) or methionine (Met, M) residues. This is also a common PTM observed in proteins and peptides. Oxidation of methionine occurs in mAbs during purification, formulation, and storage processes, and it can decrease bioactivity and stability of IgGs, which results in reduced product serum half-life and limited shelf-life.[13] Oxidation can also occur from frequent freeze-thawing cycles. In vivo oxidation is caused by oxygen radicals and other biological factors (e.g., exposure to certain oxidizing drugs or other compounds). In vitro oxidation can be due to conditions encountered during purification or formulation. Protein chemists in process development and quality control are concerned with oxidation as it can adversely impact the activity and stability of biotherapeutics.[14] The studied mAb products and biosimilars showed low oxidation levels (<2.81%). Residue M256/M255, which is potentially susceptible to oxidation (Figure 8), was a common modification for all the four studied mAbs, showing the highest levels for rituximab DP (2.81%) and trastuzumab BS (2.79%).

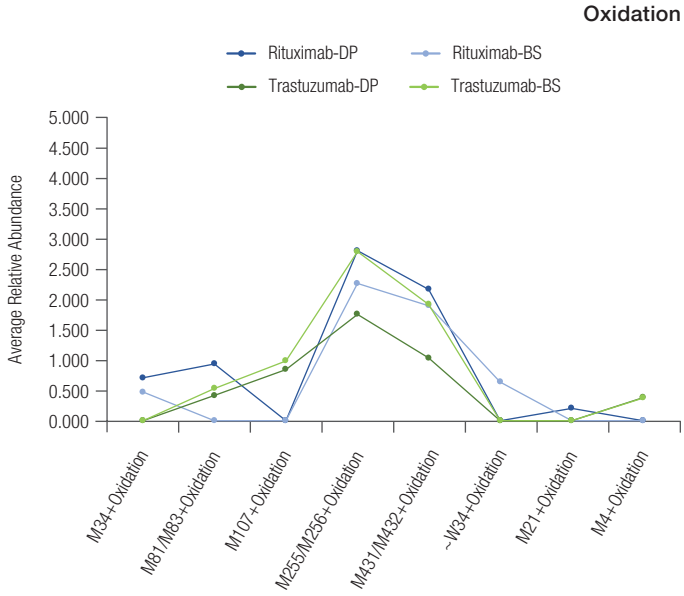


**Figure 8. Average relative abundance (n=3) of eight identified oxidation modifications for rituximab and trastuzumab drug products and biosimilars produced in-house by CHO expression systems**

Some of the most noted PTMs for therapeutic mAbs are their varied N-linked glycan structures, which include galactosylation, fucosylation, mannosylation, and sialylation. Glycosylation is a highly variable and heterogeneous process that depends on such factors as clonal variation, production cell line, media and culture conditions.[15-17] Their characterization and quantification are critical to ascertain therapeutic efficacy and safety of the drug. *N*-glycans have important structural functions as they stabilize the CH2 domain of IgGs. Deglycosylation makes mAbs thermally less stable and more susceptible to unfolding and aggregate formation. Moreover, functionality of the IgG is influenced by the attached *N*-glycans and their size.[18] MAbs produced by CHO cells typically have complex biantennary structures with no bisecting *N*-acetylglucosamine (GlcNAc) and a high level of core fucosylation. Overexpression of *N*-acetylglucosaminetransferase III in such cell lines increases bisecting GlcNAc and nonfucosyated oligosaccharides on mAbs, and thus raises antibody-dependent, cell-mediated cytotoxicity (ADCC).[19]

High abundance of glycosylation of the heavy chain is also observed for the four studied mAb products on the Fc region at position N301 (rituximab DP and BS) or N300 (trastuzumab DP and in-house produced trastuzumab biosimilar expressed by CHO cell line). The main glycans are complex biantennary oligosaccharides containing from 0 to 2 non-reducing galactoses with fucose attached to the reducing end of *N*-acetylglucosamine (A2G0F, A2G1F, A2G2F, A1G0F and A1G1F). Also present are afucosylated biantennary (A1G0 and A2G0) and high mannose (M5, M6, M7, and M8) structures (Figure 9). Core fucosylation is relatively quantified between 63.35% and 97.20% for rituximab BS and rituximab DP, respectively, and between 79.04% and 87.98% for trastuzumab BS and DP, respectively.

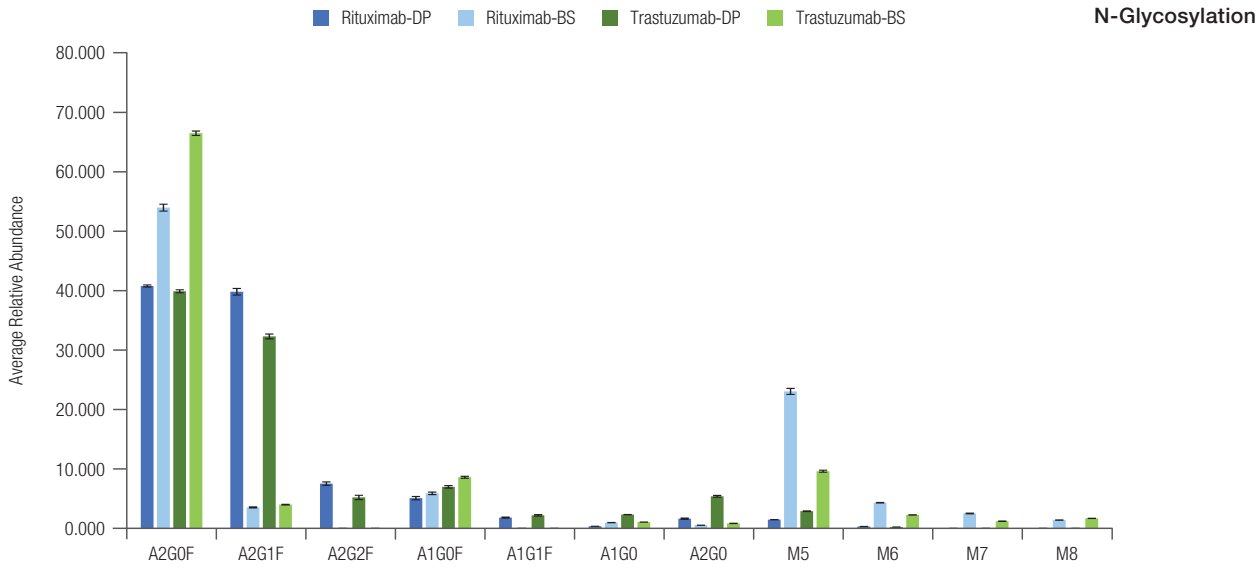


**Figure 9. Average relative abundance (n=3) of identified *N*-glycosylation on the Fc region for rituximab and trastuzumab drug products and biosimilars produced in-house by CHO expression systems**

Glycosylation of the Fc region is also important for maintaining a long catabolic half-life.[20] IgGs containing high-mannose glycans have shown increased serum clearance.[21] In addition, terminal sialic acid leads to upregulation of the surface expression of the FcγRIIb on inflammatory cells, thereby initiating the anti-inflammatory cascade.[22] Mannose-5 (M5) is detected in higher abundance for rituximab BS (23.03%) and trastuzumab BS (9.60%) CHO expressed in-house, also showing noticeable levels of higher mannose structures such as M6 (4.30-2.25%), M7 (2.50-1.19%), and M8 (1.38-1.67%), which have not been detected for DP (Tables 9 and 10). According to the literature, high levels of M5 were observed during development of a therapeutic mAb produced in a CHO cell line and correlated to the increase of cell culture medium osmolality levels and culture duration.[23] *N*-acetylneuraminic acid (Neu5Ac or NANA) is detected only in the rituximab and trastuzumab DPs at low levels < 1.7%. Figure 10 shows the normalized comparison between high mannose, non-galactosylated, and galactosylated glycans relatively quantified for the four studied mAbs. Non-galactosylated biantennary *N*-glycan structures are detected with highest relative abundance (51.10% and 63.84% for rituximab DP and BS, respectively, and 57.70% and 80.45% for trastuzumab DP and BS, respectively). Highest levels of galactosylation are detected for rituximab DP (47.06%) and trastuzumab DP (39.20%), while BS showed levels between 3.66% (rituximab BS) and 4.16% (trastuzumab BS). Regarding high mannose content, there is a noticeable variability between the four studied samples. Rituximab DP and trastuzumab DP contained the lowest high mannose content (1.84% and 3.10%, respectively) and biosimilars showed the highest levels (32.50% and 15.38%, respectively).

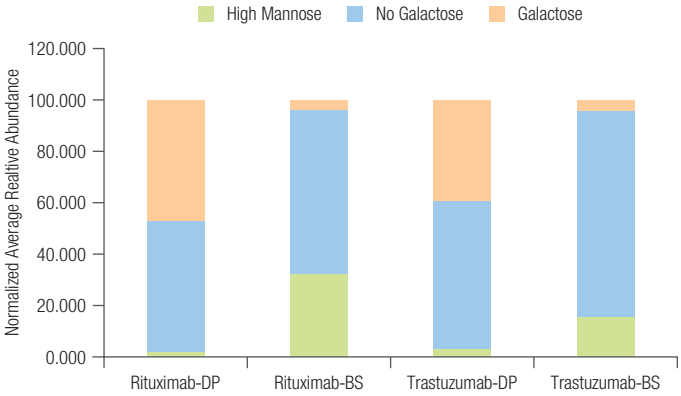


**Figure 10. Normalized average relative abundance (n=3) of identified high-mannose, non-galactosylated, and galactosylated *N*-glycans for rituximab and trastuzumab drug products and two biosimilars produced in-house by CHO and HEK expression systems, respectively**

The C-terminal lysine (Lys) variants are a very common phenomenon observed in monoclonal antibodies and recombinant proteins. Although the effect that this variation has on protein activity does not seem to impact potency or safety profile[24], the degree of heterogeneity of C-terminal Lys variants reflect the manufacturing consistency and should be monitored for product consistency. Lys loss is detected in the four studied samples at different levels (Tables 9 and 10), with the lowest % of modification for rituximab BS (90.62%) and the highest level of modification detected for trastuzumab BS (97.86%).

Other commonly targeted modifications are lysine (K) glycations, sites of which are listed in Tables 9 and 10. In total, between 13 lysine glycations could be identified and relatively quantified for rituximab DP (<0.69%) and BS (< 1.84%) for K148 site. Interestingly, trastuzumab showed 18 lysine glycations with the highest levels for DP K325 residue (1.58%) and trastuzumab BS showed levels <1.63% (K39).

**Table 9. Comparison of the deamidation, oxidation, glycation, lysine-loss and glycosylation modifications identified for rituximab drug product and biosimilar studied (n=3)**

| Protein | Modification | Rituximab DP (n=3) | Rituximab DP, RSD (n=3) | Rituximab BS (n=3) | Rituximab BS, RSD (n=3) |
|---|---|---|---|---|---|
| Heavy chain | Q1+Gln->Pyro-Glu | 99.919 | 0.002 | 95.2249 | 0.097 |
| Light chain | Q1+Gln->Pyro-Glu | 85.693 | 1.158 | 70.5048 | 0.156 |
| Heavy chain | N33+Deamidation | 0.439 | 5.608 | 0.737 | 2.547 |
| Heavy chain | N55+Deamidation | 7.067 | 7.666 | 8.512 | 0.561 |
| Heavy chain | N163+Deamidation | 0.457 | 4.674 | - | - |
| Heavy chain | N290+Deamidation | 0.520 | 1.756 | 0.485 | 3.184 |
| Heavy chain | N301+Deamidation | 0.095 | 2.323 | - | - |
| Heavy chain | N319+Deamidation | 1.950 | 11.737 | 1.663 | 2.043 |
| Heavy chain | N365+Deamidation | 1.211 | 3.802 | 1.091 | 2.250 |
| Heavy chain | Q366+Deamidation | 0.273 | 4.272 | - | - |
| Heavy chain | ~N393+Deamidation | 2.489 | 7.556 | 2.391 | 2.723 |
| Heavy chain | ~Q423+Deamidation | 0.551 | 12.770 | - | - |
| Heavy chain | ~N438+Deamidation | 1.300 | 9.579 | - | - |
| Light chain | ~Q36+Deamidation | 0.224 | 3.650 | - | - |
| Light chain | ~Q88+Deamidation | 0.387 | 12.866 | - | - |
| Light chain | ~N136+Deamidation | 0.711 | 4.549 | 0.401 | 5.397 |
| Light chain | Q146+Deamidation | 0.285 | 3.753 | - | - |
| Light chain | ~Q159+Deamidation | 0.319 | 12.837 | - | - |
| Light chain | Q198+Deamidation | 0.071 | 5.828 | - | - |
| Heavy chain | M34+Oxidation | 0.706 | 6.209 | 0.472 | 10.046 |
| Heavy chain | M81+Oxidation | 0.938 | 6.038 | - | - |
| Heavy chain | M256+Oxidation | 2.805 | 1.457 | 2.264 | 1.181 |
| Heavy chain | M432+Oxidation | 2.168 | 4.135 | 1.896 | 2.578 |
| Light chain | ~W34+Oxidation | - | - | 0.639 | 6.734 |
| Light chain | M21+Oxidation | 0.203 | 12.689 | - | - |
| Heavy chain | K63+Glycation | - | - | 0.577 | 5.216 |
| Heavy chain | K137+Glycation | 0.302 | 9.471 | 0.678 | 1.589 |
| Light chain | K144+Glycation | - | - | 0.247 | 3.471 |
| Light chain | K148+Glycation | 0.690 | 12.726 | 1.842 | 3.109 |
| Light chain | K182+Glycation | 0.458 | 7.301 | 1.437 | 3.466 |
| Light chain | K187+Glycation | 0.585 | 3.770 | 0.766 | 6.013 |

Table 9 (Continued). Comparison of the deamidation, oxidation, glycation, lysine-loss and glycosylation modifications identified for rituximab drug product and biosimilar studied (n=3)

| Protein | Modification | Rituximab DP (n=3) | Rituximab DP, RSD (n=3) | Rituximab BS (n=3) | Rituximab BS, RSD (n=3) |
|---|---|---|---|---|---|
| Light chain | K189+Glycation | 0.077 | 10.802 | - | - |
| Light chain | K206+Glycation | - | - | 0.282 | 4.052 |
| Heavy chain | K451+Lys Loss | 96.512 | 0.037 | 90.623 | 0.163 |
| Heavy chain | N301+A1G0 | 0.342 | 5.911 | 0.953 | 1.953 |
| Heavy chain | N301+A1G0F | 5.062 | 2.841 | 5.879 | 1.740 |
| Heavy chain | N301+A1G1F | 1.797 | 11.967 | - | - |
| Heavy chain | N301+A1S1F | 0.208 | 1.153 | - | - |
| Heavy chain | N301+A2G0 | 1.611 | 3.774 | 0.517 | 2.163 |
| Heavy chain | N301+A2G0F | 40.775 | 0.845 | 53.956 | 1.128 |
| Heavy chain | N301+A2G1 | 0.632 | 0.804 | - | - |
| Heavy chain | N301+A2G1F | 39.803 | 2.049 | 3.516 | 2.270 |
| Heavy chain | N301+A2G2F | 7.511 | 2.256 | - | - |
| Heavy chain | N301+A2S1G0F | 0.483 | 8.957 | - | - |
| Heavy chain | N301+A2S1G1F | 1.005 | 11.177 | - | - |
| Heavy chain | N301+A2S2F | 0.478 | 10.156 | - | - |
| Heavy chain | N301+A3G0F | - | - | 1.287 | 1.071 |
| Heavy chain | N301+A3G1F | 0.157 | 3.359 | - | - |
| Heavy chain | N301+Gn | - | - | 1.698 | 3.072 |
| Heavy chain | N301+M5 | 1.454 | 0.280 | 23.031 | 2.023 |
| Heavy chain | N301+M6 | 0.295 | 7.111 | 4.304 | 1.622 |
| Heavy chain | N301+M7 | - | - | 2.498 | 3.177 |
| Heavy chain | N301+M8 | - | - | 1.378 | 2.631 |
| Heavy chain | N301+Unglycosylated | 1.336 | 17.487 | 1.383 | 2.322 |
| Heavy chain | N301+M8 | - | - | 1.378 | 2.631 |
| Heavy chain | N301+Unglycosylated | 1.336 | 17.487 | 1.383 | 2.322 |

Table 10. Comparison of the deamidation, oxidation, glycation, lysine-loss, and glycosylation modifications identified for trastuzumab drug product and biosimilar studied (n=3)

| Relative Abundance (%) | | | | | |
|---|---|---|---|---|---|
| Protein | Modification | Trastuzumab DP (n=3) | Trastuzumab DP, RSD (n=3) | Trastuzumab BS (n=3) | Trastuzumab BS, RSD (n=3) |
| Heavy chain | ~Q3+Deamidation | - | - | 0.367 | 7.097 |
| Heavy chain | ~Q13+Deamidation | 0.299 | 14.640 | - | - |
| Heavy chain | N28+Deamidation | 0.051 | 10.428 | - | - |
| Heavy chain | N55+Deamidation | 1.693 | 2.128 | 1.766 | 2.797 |
| Heavy chain | N77+Deamidation | 0.662 | 1.892 | 0.650 | 6.166 |
| Heavy chain | Q82+Deamidation | 0.242 | 15.735 | - | - |
| Heavy chain | N84+Deamidation | 1.340 | 6.104 | 1.006 | 3.116 |
| Heavy chain | N289+Deamidation | 0.264 | 5.494 | 0.486 | 7.237 |
| Heavy chain | N300+Deamidation | 0.073 | 5.561 | - | - |
| Heavy chain | N318+Deamidation | 1.937 | 11.390 | 1.756 | 6.373 |
| Heavy chain | N328+Deamidation | 2.545 | 4.699 | - | - |
| Heavy chain | N364+Deamidation | 1.164 | 4.098 | 1.211 | 10.634 |
| Heavy chain | Q365 +Deamidation | 0.154 | 15.557 | 0.155 | 6.031 |
| Heavy chain | N387+Deamidation | 2.376 | 3.210 | - | - |
| Heavy chain | ~N392+Deamidation | - | - | 2.662 | 7.500 |
| Heavy chain | ~Q422+Deamidation | 0.295 | 13.616 | 0.057 | 8.849 |
| Heavy chain | N437+Deamidation | 1.191 | 6.289 | - | - |
| Light chain | Q27+deamidation | 5.626 | 3.511 | - | - |
| Light chain | N30+Deamidation | 3.087 | 6.181 | 9.392 | 2.672 |
| Light chain | Q38+Deamidation | 0.222 | 9.985 | - | - |
| Light chain | ~N137+Deamidation | 0.608 | 2.685 | 0.638 | 8.896 |
| Light chain | Q199+Deamidation | 0.064 | 19.876 | - | - |
| Heavy chain | M83+Oxidation | 0.415 | 2.390 | 0.532 | 6.138 |
| Heavy chain | M107+Oxidation | 0.844 | 3.392 | 0.986 | 12.728 |

Table 10 (Continued). Comparison of the deamidation, oxidation, glycation, lysine-loss, and glycosylation modifications identified for trastuzumab drug product and biosimilar studied (n=3)

| Relative Abundance (%) | | | | | |
|---|---|---|---|---|---|
| Protein | Modification | Trastuzumab DP (n=3) | Trastuzumab DP, RSD (n=3) | Trastuzumab BS (n=3) | Trastuzumab BS, RSD (n=3) |
| Heavy chain | M431+Oxidation | 1.034 | 8.911 | 1.920 | 3.982 |
| Heavy chain | M361+Oxidation | 0.164 | 8.929 | - | - |
| Light chain | M4+Oxidation | 0.381 | 8.610 | 0.377 | 8.366 |
| Heavy chain | K30+Glycation | 0.820 | 1.723 | 1.392 | 2.858 |
| Heavy chain | K76+Glycation | 0.179 | 6.451 | 0.176 | 3.391 |
| Heavy chain | K136+Glycation | 0.497 | 5.148 | 0.697 | 2.198 |
| Heavy chain | K251+Glycation | 0.088 | 9.273 | - | - |
| Heavy chain | ~K291+Glycation | 0.482 | 2.329 | 0.673 | 0.699 |
| Heavy chain | K293+Glycation | 0.116 | 8.646 | - | - |
| Heavy chain | K320+Glycation | 0.820 | 1.723 | 0.183 | 2.320 |
| Heavy chain | K323+Glycation | 0.104 | 9.495 | - | - |
| Heavy chain | K325+Glycation | 1.580 | 12.067 | - | - |
| Heavy chain | K329+Glycation | 0.450 | 0.314 | 0.949 | 2.430 |
| Heavy chain | K337+Glycation | 0.063 | 3.309 | - | - |
| Heavy chain | K363+Glycation | 0.080 | 6.908 | - | - |
| Light chain | K39+Glycation | - | - | 1.631 | 11.126 |
| Light chain | K103+Glycation | 1.152 | 1.359 | 1.540 | 2.365 |
| Light chain | K149+Glycation | 0.919 | 4.916 | 1.602 | 3.077 |
| Light chain | K169+Glycation | - | - | 0.454 | 4.923 |
| Light chain | K183+Glycation | 0.369 | 13.651 | 1.044 | 3.594 |
| Light chain | K188+Glycation | 0.939 | 6.465 | - | - |
| Light chain | K190+Glycation | 0.113 | 4.871 | - | - |
| Heavy chain | K450+Lys Loss | 97.730 | 0.098 | 97.859 | 0.037 |
| Heavy chain | N300+A1G0 | 2.297 | 2.306 | 1.037 | 0.758 |
| Heavy chain | N300+A1G0F | 6.976 | 9.383 | 8.582 | 1.906 |
| Heavy chain | N300+A1G1 | 0.594 | 1.401 | - | - |
| Heavy chain | N300+A1G1F | 2.180 | 6.721 | - | - |
| Heavy chain | N300+A1S1 | 0.091 | 5.173 | - | - |
| Heavy chain | N300+A1S1F | 0.401 | 2.875 | - | - |
| Heavy chain | N300+A1G1M4F | - | - | 0.470 | 1.573 |
| Heavy chain | N300+A2G0 | 5.378 | 1.718 | 0.820 | 3.669 |
| Heavy chain | N300+A2G0F | 39.879 | 0.616 | 66.477 | 0.559 |
| Heavy chain | N300+A2G1 | 1.938 | 0.475 | - | - |
| Heavy chain | N300+A2G1F | 32.283 | 2.911 | 3.979 | 1.523 |
| Heavy chain | N300+A2G2 | 0.165 | 1.872 | - | - |
| Heavy chain | N300+A2G2F | 5.190 | 3.141 | - | - |
| Heavy chain | N300+A2S1G0F | 0.442 | 10.083 | - | - |
| Heavy chain | N300+A2S1G1F | 0.647 | 1.787 | - | - |
| Heavy chain | N300+A2S2F | 0.234 | 6.664 | - | - |
| Heavy chain | N300+A3G0F | - | - | 2.087 | 2.550 |
| Heavy chain | N300+A3G1F | 0.161 | 4.784 | - | - |
| Heavy chain | N300+Gn | 0.069 | 6.463 | 1.115 | 3.428 |
| Heavy chain | N300+M3 | 0.165 | 17.312 | - | - |
| Heavy chain | N300+M4 | 0.153 | 0.493 | - | - |
| Heavy chain | N300+M5 | 2.874 | 2.319 | 9.603 | 1.772 |
| Heavy chain | N300+M6 | 0.204 | 3.781 | 2.246 | 1.167 |
| Heavy chain | N300+M7 | - | - | 1.189 | 2.799 |
| Heavy chain | N300+M8 | - | - | 1.005 | 0.441 |
| Heavy chain | N300+M9 | - | - | 0.322 | 3.394 |
| Heavy chain | N300+Unglycosylated | 1.443 | 4.976 | 1.668 | 1.375 |

## Conclusions

- The Magnetic SMART Digest kit provides simple, automated, rapid protein digestion for peptide mapping analysis and PTM quantification for comparability studies between innovator and biosimilar monoclonal antibodies.

- Analysis of chimeric and humanized mAbs samples gave excellent quality data with high confidence in results. Excellent sequence coverage (~100%) and good reproducibility of post-translational modifications were observed with Magnetic SMART Digest protocol.

- Peptide mapping was easily automated, resulting in less sample handling, increased productivity, and improved reproducibility, even with peptides at low levels. This will allow confident transfer of methods between laboratories.

- Biosimilarity of the primary structure for both rituximab and trastuzumab BS products and their respective PTMs were achieved successfully by this analytical approach using automated magnetic SMART digestion for peptide generation and subsequent LC-MS analysis. The Thermo Scientific™ peptide mapping workflow provided reproducible results with excellent mass accuracy and high sensitivity.

- The BioPharma Finder 3.0 software can provide automatic data processing, peptide sequence matching, and protein sequence coverage mapping accurately and with high confidence.

## References


1. Chaudhari, P.S.; Nath, R and Gupta, S.K. Opportunities and challenges in biosimilar development. *Bioprocess International*, **2017**, *15* (5), 24-33.
2. EMA. *Biosimilars in the EU, Information guide for healthcare professionals*. EMA 2017.
3. EMA. European public assessment reports (EPAR) for human medicines. Available at https://data.europa.eu/euodp/es/data/dataset/epar-human-medicines. 2016. Accessed February 9, 2018.
4. Mendoza-Mancedo, K.; Romero-Díaz, A.; Miranda-Hernández, M.P. et al. Characterization and comparability of biosimilars: a filgrastim case of study and regulatory perspectives for Latin America. *Electronic Journal of Biotechnology*, **2016**, *24*, 63-69.
5. FDA-CDER-CBER. Quality Considerations in Demonstrating Biosimilarity of a Therapeutic Protein Product to a Reference Product. *Guidance for Industry*. April 2015.
6. McCamish, M.; Woollett, G. The rise of the biosimilars. *Expert Review of Clinical Pharmacology*, **2012**, *5*, 597-599.
7. Derbyshire M. Patent expiry dates for biologicals: 2017 update. *Generics and Biosimilars Initiative Journal* (GaBI Journal). **2018**, *7*(1), 29-34.
8. Slamon, D.J.; Leyland-Jones, B.; Shak, S. et al. Use of chemotherapy plus a monoclonal antibody against HER2 for metastatic breast cancer that overexpresses HER2. *The New England Journal of Medicine*, **2001**, *344*(11), 783-792.
9. Tsuruta, L. R.; Lopes dos Santos, M. Biosimilars Advancements: Moving on to the Future. *Biotechnology Progress*, **2015**, *31*(5), 1139-1149.
10. EMA/CHMP/437/04. *Guideline on Similar Biological Medicinal Products*. Available at: http://www.ema.europa.eu/docs/en_GB/document_library/Scientific_guideline/2009/09/WC500003517.pdf. October 2005.
11. Vlasak, J.; Bussat, M. C.; Wang, S. et al. Identification and characterization of asparagine deamidation in the light chain CDR1 of a humanized IgG1 antibody. *Analytical Biochemistry*, **2009**, *392*, 145–154.
12. Liu, H.; Gaza-Bulseco, G.; Chumsae, C. Glutamine deamidation of a recombinant monoclonal antibody. *Rapid Communications in Mass Spectrometry*, **2008**, *22*(24), 4081-4088.
13. Wang, W.; Vlasak, J.; Li, Y. et al. Impact of methionine oxidation in human IgG1 Fc on serum half-life of monoclonal antibodies. *Molecular Immunology*, **2011**, *48*, 860–866.
14. Haberger, M.; Heidenreich, A.K.; Schlothauer, T. et al. Functional assessment of antibody oxidation by native mass spectrometry. *MABS*, **2015**, *0:0*, 1-10.
15. Patel T.P. et al. Different Culture Methods Lead to Differences in Glycosylation of a Murine IgG Monoclonal Antibody. *Biochemistry Journal*, **1992**, *285*(Pt 3), 839–845.
16. Schmelzer A.E. and Miller W.M. Hyperosmotic Stress and Elevated pCO2 Alter Monoclonal Antibody Charge Distribution and Monosaccharide Content. *Biotechnology Progress*, **2002**, *18*(2), 346–353.
17. Zeck A, et al. Cell Type-Specific and Site Directed N-Glycosylation Pattern of FcgammaRIIIa. *Journal of Proteome Research*, **2011**, *10*(7), 3031–3039.
18. Higel, F.; Seidl, A.; Sorgel, F.; Friess, W. N-glycosylation heterogeneity and the influence on structure, function and pharmacokinetics of monoclonal antibodies and Fc fusion proteins. *European Journal of Pharmaceutics and Biopharmaceutics*, **2016**, *100*, 94-100.
19. Yamane-Ohnuki N, Satoh M. Production of Therapeutic Antibodies with Controlled Fucosylation. *MABS*, **2009**, *1*(3), 230–236.
20. Jones A.J. et al. Selective Clearance of Glycoforms of a Complex Glycoprotein Pharmaceutical Caused By Terminal N-Acetylglucosamine Is Similar in Humans and Cynomolgus Monkeys. *Glycobiology*, **2007**, *17*(5), 529–540.
21. Goetze A.M. et al. High-Mannose Glycans on the Fc Region of Therapeutic IgG Antibodies Increase Serum Clearance in Humans. *Glycobiology*, **2011**, *21*(7), 949–059.
22. Anthony R.M.; Ravetch J.V. A Novel Role for the IgG Fc Glycan: The Anti-Inflammatory Activity of Sialylated IgG Fcs. *Journal of Clinical Immunology*, **2010**, *30* (Sup 1), S9 S14.
23. Pacis, E.; Yu, M.; Autsen, J.; Bayer, R.; Li, F. Effects of cell culture conditions on antibody N-linked glycosylation- What affects high mannose 5 glycoform. *Biotechnology and Bioengineering*, **2011**, *108*, 2348–2358.s
24. Dick, L.W.; Qiu, D.; Mahon, D. et al. C-terminal Lysine variants in fully human monoclonal antibodies: investigation of test methods and possible causes. *Biotechnology and Bioengineering*, **2008**, *100*(6), 1132-1143.


Find out more at **thermofisher.com/peptidemaps**



ThermoFisher SCIENTIFIC